

General Disclaimer

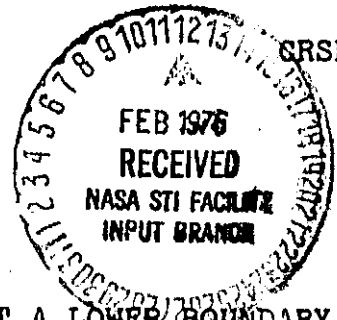
One or more of the Following Statements may affect this Document

- This document has been reproduced from the best copy furnished by the organizational source. It is being released in the interest of making available as much information as possible.
- This document may contain data, which exceeds the sheet parameters. It was furnished in this condition by the organizational source and is the best copy available.
- This document may contain tone-on-tone or color graphs, charts and/or pictures, which have been reproduced in black and white.
- This document is paginated as submitted by the original source.
- Portions of this document are not fully legible due to the historical nature of some of the material. However, it is the best reproduction available from the original submission.

CORNELL UNIVERSITY

Center for Radiophysics and Space Research

ITHACA, N. Y.



CRSR 616

JOVIAN METEOROLOGY:

LARGE-SCALE MOIST CONVECTION WITHOUT A LOWER BOUNDARY

(NASA-CR-146353) JOVIAN METEOROLOGY: N76-17034
LARGE-SCALE MOIST CONVECTION WITHOUT A LOWER
BOUNDARY (Cornell Univ.) 37 p HC \$4.00

CSCI 3B Unclass
G3/91 13529

Peter J. Gierasch



JOVIAN METEOROLOGY:
LARGE-SCALE MOIST CONVECTION WITHOUT A LOWER BOUNDARY

Peter J. Gierasch

Center for Radiophysics and Space Research
Ithaca, N.Y. 14853

November 1975

ABSTRACT

It is proposed that Jupiter's cloud bands represent large scale convection whose character is determined by the phase change of water at a level where the temperature is about 275K. It is argued that there are three important layers in the atmosphere: a tropopause layer where emission to space occurs, an intermediate layer between the tropopause and the water cloud base, and the deep layer below the water cloud. The barotropic behavior observed in the visible clouds is seated in the tropopause layer where the stability is large. Horizontal potential temperature contrasts in the intermediate layer are larger than vertical ones, are given by the difference between moist and dry adiabats, and produce the observed thermal winds. Horizontal temperature contrasts in the deep layer are extremely small, and ordinary convection exists, with an unstable potential temperature gradient. The intermediate layer is stably stratified.

It is argued that such a structure would spontaneously develop on a radiative time scale from an initial horizontally uniform convective state, and that the belt-zone spacing would be determined by the barotropic stability criterion, as Ingersoll and Cuzzi (1969) suggested. All arguments are only semi-quantitative, since convection in a deep atmosphere or with phase changes is not understood. A major purpose is to point out that these ingredients are essential to Jovian meteorology.

I. Introduction

This paper outlines a theory of the Jovian general circulation. Latent heat release in water clouds and the lack of a lower boundary to the atmosphere are central to the theory. The discussion is largely qualitative, because our understanding of the dynamical effects of phase changes and great depth is poor. A major purpose of the paper is to argue that further work in these areas is necessary to understand Jupiter's atmosphere, even to a qualitative first approximation.

The arguments fall into three major categories, as follows:

1) The observed wind speeds and belt spacings are consistent with an adiabatic structure varying between moist and dry in zones and belts. Ingersoll and Cuzzi (1969) showed that Peek's (1958) data on latitude variation of rotation period is consistent with winds satisfying the thermal wind equation (hydrostatic balance in the vertical and coriolis force balancing pressure gradient in the horizontal), with a fixed level of no motion at some depth and a fixed temperature difference between belts and zones. Barcilon and Gierasch (1970) showed that the data is consistent with the fixed level being the water cloud base and with the fixed temperature difference being the variation between the moist and dry adiabats, if the water abundance is given by the solar O:H ratio.

2) A hypothetical initial convective configuration, horizontally uniform on the belt-zone scale, would be unstable on a radiative

time scale to development of zones and belts. The reason is that the onset of a large circulation cell would quench moist convection at downwelling locations, leading to radiative cooling of the layer between the level of emission to space (tropopause layer) and the water cloud base. Gierasch, Ingersoll, and Williams (1973) have shown that such a correlation between vertical displacement and radiative cooling can produce an instability leading to amplification of the initial displacement. The time scale would be on the order of 10^8 s, consistent with observed variations in the large scale structure.

3) The observed barotropic behavior of motions is consistent with a stable tropopause layer at the top of the atmosphere, and an intermediate weakly stable layer between the water cloud base and the tropopause layer. It has been suspected for some time that the Jovian cloud motions are controlled by two-dimensional vorticity conservation (Ingersoll and Cuzzi, 1969). Striking qualitative confirmation now exists (Williams, 1975; Maxworthy, 1975; Ingersoll, 1973). We argue that such behavior is to be expected if the Rossby number ϵ satisfies $\epsilon \ll 1$, if in the tropopause layer $\epsilon^2 Ri \gg 1$ (where Ri is the Richardson number), and if $\epsilon^2 Ri \ll 1 < Ri$ in the intermediate layer. We also argue that the moisture-related instability should lead to this structure.

These points are not treated in this order, or even systematically one at a time. It is more convenient, following the equations of motion, to treat short time scales first (Section II), and then long time scales (Section III). In Section IV the uniqueness of Jupiter and applications to the other outer planets are discussed.

An excellent and comprehensive review paper has just been written by Stone (1975) and it is not necessary for us to discuss previous theoretical modeling here in any detail. Realistic treatment of vertical structure has not been attempted. An artificial lower boundary has generally been assumed, removing the coupling to deep layers which exists on the real planet. The consequences are both thermal and dynamical. Deep layers are almost certainly very close to horizontally isothermal (Bogart and Gierasch, 1976) and a boundary removes the constraint that should be imposed on the atmosphere. A boundary has the dynamical effect of permitting horizontal pressure gradients to exist at the base. We comment further on this in Section II. The other deficiency in previous work has been neglect of latent heat release. On Jupiter this is one of the largest potential sources for horizontal temperature variation.

An exception is the work by Barcilon and Gierasch (1970). An attempt was made to treat both latent heat and coupling to deep levels. However, the discussion was based on a highly idealized axisymmetric steady flow, with a frictionally controlled meridional circulation. No attempt was made to explain self-consistently the origin of the flow or its scale.

We shall make several basic assumptions throughout this paper. One is that the abundance of water on Jupiter is given to correct order of magnitude by the solar O:H ratio. For levels of cloud condensation on different planets we refer to Weidenschilling and Lewis (1973). We assume that condensation of water leads to precipitation, so that there is differentiation

between dry and moist gas. This is discussed by Rossow and Gierasch (1976). We assume the ideal gas equation of state. We use locally cartesian geometry (a β -plane), since the scale of the belts and zones is much less than the radius of the planet.

II. Short Time Scales

In this section we discuss motions whose time scales are on the order of L/U , where U is the order of the flow speed and L is the characteristic horizontal scale. The important motions in this category are the shear instabilities at cloud level, and other instabilities that might exist at other levels.

The length scale $L \sim D/2\pi$, where D is the spacing between zones. With $D = 10^9$ cm and $U = 25 \text{ ms}^{-1}$ (consistent with a differential rotation period of about one minute) we obtain the time scale $L/U \sim 10^5$ s. We assume that friction, radiative heating, and eddy diffusion are negligible on this time scale. We shall also assume that the depth of the flow is much less than L , so that the hydrostatic approximation is valid. The equations in pressure coordinates are

$$\frac{Du}{Dt} - fv + \frac{\partial \phi}{\partial x} = 0 \quad (1)$$

$$\frac{Dv}{Dt} + fu + \frac{\partial \phi}{\partial y} = 0 \quad (2)$$

$$\frac{\partial \phi}{\partial p} = -\frac{R}{p} \left(\frac{p}{p_0} \right)^{\kappa} \ominus, \quad (3)$$

$$\frac{\partial u}{\partial x} + \frac{\partial v}{\partial y} + \frac{\partial \omega}{\partial p} = 0, \quad (4)$$

$$\frac{D \ominus}{Dt} = 0, \quad (5)$$

where

$$\Theta = \left(\frac{p_0}{p}\right)^\kappa T, \quad \kappa = \frac{\gamma-1}{\gamma}, \quad f = f_0 + \beta y,$$

and the notation is

- x, y = eastward, northward directions,
 u, v = x, y velocities,
 p, ω = pressure, Dp/Dt ,
 t = time,
 D/Dt = $\partial/\partial t + u\partial/\partial x + v\partial/\partial y + w\partial/\partial p$,
 ϕ = geopotential height,
 γ, R = specific heat ratio, gas constant,
 T, Θ = temperature, potential temperature,
 p_0 = reference pressure (water cloud base)
 f_0, β = coriolis parameter, and its gradient.

Let Θ and ϕ be written as a static part plus a part associated with dynamics:

$$\Theta = \theta_s(p) + \theta(x, y, p, t) \quad (6)$$

$$\phi = \phi_s(p) + \phi(x, y, p, t) \quad (7)$$

Let the amplitude $\Delta\theta$ be associated with θ . Define

$$\epsilon = \frac{U}{f_0 L}, \quad S = \frac{p_0}{\Delta\theta} \frac{d\theta_s}{dp}, \quad B = \frac{\beta L}{f_0}. \quad (8)$$

Note that $S(p)$ is a function of depth; ϵ and B are not.

Nondimensionalize as follows:

$$\begin{array}{ll}
 \theta \text{ by } \Delta\theta, & x, y, p \text{ by } L, L, p_0 \\
 \phi \text{ by } R\Delta\theta, & t \text{ by } U/L, \\
 u, v \text{ by } R\Delta\theta/f_0 L = U, & \omega \text{ by } p_0 U/L.
 \end{array} \quad (9)$$

Equations (1) - (5) become, in terms of dimensionless variables,

$$\epsilon \frac{Du}{Dt} - (1 + By)v + \frac{\partial \phi}{\partial x} = 0 \quad (10)$$

$$\epsilon \frac{Dv}{Dt} + (1 + By)u + \frac{\partial \phi}{\partial y} = 0 \quad (11)$$

$$\frac{\partial \phi}{\partial p} = - \frac{\theta}{p^{1-\kappa}} \quad (12)$$

$$\frac{\partial u}{\partial x} + \frac{\partial v}{\partial y} + \frac{\partial \omega}{\partial p} = 0 \quad (13)$$

$$\frac{D\theta}{Dt} + S\omega = 0 \quad (14)$$

We proceed by expanding in ϵ , as is usual in developing quasi-geostrophic theory. Observationally, $U \sim 25 \text{ ms}^{-1}$, $L \sim 2 \times 10^8 \text{ cm}$, and $f_0 \sim 2 \times 10^{-4} \text{ s}^{-1}$, so that $\epsilon \sim 1/16$. Let $b = B/c$; observationally, b is order unity. Write all dependent variables as a power series in ϵ ; for example, $v = v^{(0)} + \epsilon v^{(1)} + \dots$. To leading order we obtain from (10) - (13)

$$-v^{(0)} + \frac{\partial \phi^{(0)}}{\partial x} = 0, \quad (15)$$

$$u^{(0)} + \frac{\partial \phi^{(0)}}{\partial y} = 0, \quad (16)$$

$$\frac{\partial \phi^{(0)}}{\partial p} = - \frac{\theta}{p^{1-\kappa}}, \quad (17)$$

$$\frac{\partial \omega^{(0)}}{\partial p} = 0. \quad (18)$$

We do not know how to write (14) to lowest order, since we do not know the order of S .

Going to first order in the dynamical equations (10) and (11), using (13), (15), and (16), we obtain the equation for the vertical vorticity

$$\frac{D^{(0)}}{Dt} \left(\frac{\partial v^{(0)}}{\partial x} - \frac{\partial u^{(0)}}{\partial y} + by \right) - \frac{\partial \omega^{(1)}}{\partial p} = 0, \quad (19)$$

where $D^{(0)}/Dt$ is evaluated with $u^{(0)}$, $v^{(0)}$. We have assumed the upper boundary condition $\omega^{(0)} \rightarrow 0$ as $p \rightarrow 0$; together with (18) this implies that $\omega^{(0)} = 0$. We justify this boundary condition below. Finally, (14) gives to leading order

$$\frac{D^{(0)}}{Dt} \theta^{(0)} + \epsilon S \omega^{(1)} = 0. \quad (20)$$

This completes the development of the equations, and we proceed to discuss application to Jupiter.

Rather than beginn' g by attempting to estimate the uncertain quantity S , let us first list the three qualitatively different possibilities for the system of equations (19) and (20).

1. $\epsilon S = 0(1)$. Equations (19) and (20) are coupled. This is the standard quasi-geostrophic approximation which successfully predicts the major features of mid-latitude circulation on Earth. The thermal field influences the vorticity by affecting the height of columns of fluid between isentropic surfaces, and vorticity advection affects the thermal field by causing vertical motion. When horizontal temperature gradients are present, baroclinic instabilities can develop, and the length scale of

the instabilities is internally determined to be precisely that which couples (19) and (20):

$$\epsilon S = \frac{p_0 R d \theta_s / dp}{f_0^2 L^2} = 0(1).$$

The L determined this way is called the Rossby radius of deformation.

2. $\epsilon S \gg 1$. Equation (20) predicts $\omega^{(1)} = 0$, and (19) reduces to vorticity conservation. The thermal field is secondary.

3. $\epsilon S \ll 1$. Equation (20) predicts $D^{(0)}\theta^{(0)}/Dt = 0$, (19) leads to vertical motion through vorticity advection, but the vorticity and the vertical motion field are secondary.

We propose that there is an abrupt transition in the Jovian atmosphere between $\epsilon S \gg 1$ at tropopause level and $\epsilon S \ll 1$ at deeper levels, and that the complicated intermediate regime typical of the Earth's atmosphere does not occur on Jupiter. We believe the observed barotropic behavior of the cloud motions supports this proposition. Furthermore, if one accepts the water cloud hypothesis for the origin of the horizontal temperature contrasts $\Delta\theta$, it can be argued quite reasonably that the transition will exist. Barcilon and Gierasch (1970) show that latent heat can lead to $\Delta\theta/\theta \sim 10^{-2}$. The atmosphere divides into three regions:

1. Tropopause layer. This is a layer about one scale height deep where emission to space takes place. Radiation stabilizes this layer, so that

$$\frac{p}{\theta_s} \frac{d\theta_s}{dp} \sim -1.$$

Then ϵS can be written either of two ways:

$$-\epsilon S = \epsilon \frac{p_0}{p} \frac{\theta_s}{\Delta\theta} = \frac{p_0}{p} \frac{R\theta_s}{f_0^2 L^2} \sim 10^2,$$

where we used $p_0/p \sim 14$, $R = 4 \times 10^7 \text{ erg K}^{-1} \text{ gm}^{-1}$, $\theta_s = 250 \text{ K}$, $f_0 = 1.7 \times 10^{-4} \text{ s}^{-1}$, and $L = 2 \times 10^8 \text{ cm}$.*

2. Intermediate layer. This is the region between the tropopause layer and the base of the water cloud. Since the maximum potential temperature contrast available here is $\Delta\theta$, we expect $d\theta_s/dp \lesssim -\Delta\theta/p_0$. Then

$$-\epsilon S \lesssim \epsilon.$$

3. Deep layer. This is below the water cloud. Here there are no latent heat sources, and radiation is not effective. We expect ordinary convection to exist. Mixing length theory, for example, predicts $1 \gg S > 0$.

This completes the general outline of the structure we propose. Figure 1 schematically illustrates the layers. We proceed now to a few specific remarks concerning the behavior of solutions. Discussion of the slow processes which are

* All quantities in this paragraph are dimensional, since we are evaluating ϵ and S , not using the equations of motion. For a summary of numerical values and reference to their sources, see Table 3 in Section IV.

responsible for the genesis and maintenance of the banded structure is left for Section III. Here we deal only with questions related to short term stability.

1. Conditions for a steady flow. The geostrophic and hydrostatic relations (15)-(17) can be used to solve for $u^{(0)}$ and $v^{(0)}$ in terms of $\theta^{(0)}$. If $\theta^{(0)}$ is to be steady in the intermediate layer, we must have

$$u^{(0)} \frac{\partial \theta^{(0)}}{\partial x} + v^{(0)} \frac{\partial \theta^{(0)}}{\partial y} = 0 ,$$

and therefore

$$- \frac{\partial^2 \theta^{(0)}}{\partial y \partial p} \frac{\partial \theta^{(0)}}{\partial x} + \frac{\partial^2 \theta^{(0)}}{\partial x \partial p} \frac{\partial \theta^{(0)}}{\partial y} = 0 .$$

From this it follows that the quotient $(\partial \theta^{(0)} / \partial y) / (\partial \theta^{(0)} / \partial x)$ is a function of x and y alone, and therefore that

$$\theta^{(0)} = F(p)G(x,y) , \quad (21)$$

that is, the isentropes are similar in shape at different heights.

2. Stability of the intermediate layer. It is rather difficult to imagine how the structure (21) can arise and then be maintained. We propose here that it obtains automatically because $F(p)$ is nearly constant; that is, horizontal contrasts in the potential temperature are larger than vertical ones in the intermediate

layer. The reasoning is as follows. In Section III we present a mechanism for generating horizontal temperature gradients on the belt-zone scale. Vertical gradients in the potential temperature do not arise directly. But it is well-known that in the presence of a horizontal gradient, instabilities can set in with the effect of converting some of the potential energy available because of the horizontal contrast into stable layering in the vertical. In particular, one class of instability is inertial instability, which Stone (1966, 1967, 1971) has discussed in connection with Jupiter. These are small scale instabilities which can exist locally, independent of the nature of boundary conditions (McIntyre, 1970).

Inertial instabilities grow rapidly (with a time scale on the order of τ_0^{-1}) when the Richardson number, Ri , is less than unity. Ri is given, approximately, by

$$Ri \sim \frac{\rho R \frac{d\theta}{dp}}{U^2} \sim \frac{S}{\epsilon}$$

We propose that these instabilities operate to adjust the stability so that $Ri \gtrsim 1$, and as a result, so that $S \sim \epsilon$. It is then clear from the definition of S that the ratio of vertical to horizontal potential temperature contrasts is small.

The real question is of course whether other processes or other instabilities act to stabilize the intermediate layer still further. No other instabilities are known at present to exist under these circumstances ($\epsilon \ll 1$, $Ri > 1$) in an unbounded atmosphere, but this is clearly an important question for future work.

3. Stability of the upper layer. Flow in this layer is governed by the barotropic vorticity equation, and the stability criteria should be the familiar ones for this kind of flow. For example, for a purely zonal mean flow the criterion is

$$b - \frac{\partial^2 u^{(0)}}{\partial y^2} > 0, \quad (22)$$

and this is one of the results supporting the proposition we have made.

4. Vertical motion and interaction with deep layers. In the event that barotropic instability sets in at the tropopause layer, the resulting mixing could lead to unbalanced pressure gradients which drive horizontal convergence. The horizontal "friction" caused this way would represent a breakdown in our initial assumptions.

The resulting adjustments would change the thermal structure in the intermediate layer to make it consistent with the new flow pattern at tropopause level. This process is extremely complicated, and a detailed numerical calculation would probably be required to investigate it. One question of interest, however, is the influence of such adjustments on the deep layer. Here we shall show qualitatively that the penetration depth is very large.

Combining (19) and (20) gives

$$\frac{D^{(0)}}{Dt} \left\{ \frac{\partial^2 \phi^{(0)}}{\partial x^2} + \frac{\partial^2 \phi^{(0)}}{\partial y^2} + by - \frac{\partial}{\partial p} \left[\frac{p^{1-\kappa}}{S} \frac{\partial \phi^{(0)}}{\partial p} \right] \right\} = 0. \quad (23)$$

Assume that $\phi^{(0)}$ in the deep layer is very small, so that (23) can be linearized. Let it also be proportional to $\exp(i\sigma t + i\lambda y + i\kappa x)$, i.e., Fourier analyze the disturbance. Then (23) gives

$$\frac{\partial^2 \psi}{\partial p^2} + \frac{S}{p^{1-\kappa}} \left(k^2 + \lambda^2 - \frac{\kappa b}{\sigma} \right) \psi = 0, \quad (24)$$

where

$$\psi = \frac{p^{1-\kappa}}{S} \frac{\partial \phi^{(0)}}{\partial p}.$$

Since we do not know the sign of the factor multiplying ψ in (24), we do not know if the solution decays with depth or not. In either case, the qualitative nature of the solution can be obtained by assuming that $S/p^{1-\kappa}$ is constant. The solution then gives

$$\omega^{(1)} = A \left\{ \frac{\sin}{\sinh} \right\} \left[\left| \frac{S}{p^{1-\kappa}} \left(k^2 + \lambda^2 - \frac{\kappa b}{\sigma} \right) \right|^{\frac{1}{2}} (p-p_b) \right], \quad (25)$$

$$\phi^{(0)} = \pm \frac{A}{i\sigma} \frac{S}{p^{1-\kappa}} \left\{ \frac{\cos}{\cosh} \right\} \left[\left| \frac{S}{p^{1-\kappa}} \left(k^2 + \lambda^2 - \frac{\kappa b}{\sigma} \right) \right|^{\frac{1}{2}} (p-p_b) \right], \quad (26)$$

where A is an arbitrary constant, and the choice of sign and function depends on the sign of the factor on ψ in (24). We have assumed that the correct boundary condition is $\omega^{(1)} = 0$ at some deep level $p = p_b$. We see that as long as $S \ll 1$ in the deep layer, the important results are independent of all other parameters:

a) The penetration depth for $\omega^{(1)}$ is large; if the stability S is small enough, the depth is determined by whatever interface or phase change exists to prevent motion.

b) To leading order, the boundary condition imposed on the intermediate layer by the deep layer is $\phi^{(0)} = 0$. The vertical motion $\omega^{(1)}$ is unconstrained.

III. Long Time Scales

Here we discuss slow processes whose time scale is governed by the thermal inertia of the atmosphere. This time scale is

$$t \sim \frac{c_p p_o \Delta\theta}{gF} \sim 1.3 \times 10^8 \text{ s } (\sim 4.1 \text{ yr.}),$$

where we took $c_p = 1.3 \times 10^8 \text{ erg gm}^{-1} \text{ K}^{-1}$, $p_o = 7 \times 10^6 \text{ erg cm}^{-3}$, $\Delta\theta = 1.7 \text{ K}$, $g = 2400 \text{ cm s}^{-2}$, and $F = 5 \times 10^3 \text{ erg cm}^{-2} \text{ s}^{-1}$. This is the time required for the energy flux characterizing the system to lead to temperature changes on the order of $\Delta\theta$. The important slow processes are, of course, the genesis and maintenance of the belts, zones and other permanent features of the general circulation.

Consider first a hypothetical initial state without belts or zones. The internal heat is carried by small scale convection. At very deep levels, horizontal temperature gradients are constrained to be extremely small because the superadiabaticity is small. Bogart and Gierasch (1976) have shown that for ordinary mixing length theory with rotation neglected, horizontal gradients on the order of the superadiabaticity lead to efficient horizontal redistribution of heat, so that even when an uneven heat flux is applied to the top or bottom of a deep convecting layer, horizontal temperature gradients remain small. It is unlikely that the influence of rotation in Jupiter is strong enough to change this conclusion.

The uneven heat flux applied at the top of the Jovian atmosphere by the latitude variation of the incident solar radiation therefore leads to heat redistribution at great depth, and the extremely small horizontal temperature contrasts necessary to accomplish the redistribution explain the observed lack of latitude variation in emission to space (Ingersoll et al., 1975b).

An important point is that the internal heat is large enough so that the convective heat flux exists at all latitudes. It is minimum at the equator, where the largest fraction of the emission to space is supplied by solar heat. But the ratio of total emission to total solar energy absorption would need to be less than about 1.3 for convection to cease entirely at the equator, as opposed to the observed 1.9 (Ingersoll et al., 1975a).

A few details of this hypothetical convective initial state are:

- 1) The moist and dry adiabatic lapse rates differ appreciably only in a thin layer near the water cloud (Barcilon and Gierasch, 1970). However, the latent heat may influence the nature of convection drastically by introducing larger temperature perturbations, as is the case on Earth.

- 2) Radiation is important only in the tropopause layer, where cooling to space balances the convective flux from below.

- 3) Neglecting rotation and latent heat, and assuming that the mixing length is one pressure scale height, properties of the convection are:

$$w^3 = \left(\frac{\gamma-1}{\gamma} \frac{F}{\rho_0} \right) \left(\frac{p}{p_0} \right)^{-1/\gamma}, \quad (27)$$

$$H = \frac{RT_0}{g} \left(\frac{p}{p_0} \right)^{1 - \frac{1}{\gamma}}, \quad (28)$$

$$K = wH, \quad (29)$$

$$t = H/w, \quad (30)$$

$$\frac{T'}{T} = \frac{w^2}{RT}. \quad (31)$$

where F is the convective heat flux, w is the convective velocity, p is density, a subscript zero denotes reference level (water cloud base), H is scale height, g is gravity, K is eddy diffusivity, and T' is temperature perturbation. Numerical values will be of interest, and a few are given in Table 1.

Table 1

Mixing-length convection properties

These are evaluated from (27)-(31), with $R = 3.7 \times 10^7$ erg gm⁻¹K⁻¹, $T_0 = 275$ K, $g = 2400$ cm s⁻², $\rho_0 = 7 \times 10^6$ erg cm⁻³, $\gamma = 1.4$, and $F = 5 \times 10^3$ erg cm⁻²s⁻¹.

p/p_0	w (cm s ⁻¹)	H (cm)	K (cm ² s ⁻¹)	t (s)	T'/T
0.1	4.7×10^2	2.0×10^6	9.4×10^8	4.2×10^3	4.1×10^{-6}
0.3	3.6×10^2	2.8×10^6	1.0×10^9	7.8×10^3	1.8×10^{-6}
1.0	2.7×10^2	3.9×10^6	1.1×10^9	1.4×10^4	7.2×10^{-7}
3.0	2.1×10^2	5.3×10^6	1.1×10^9	2.5×10^4	3.1×10^{-7}
10.0	1.6×10^2	7.5×10^6	1.2×10^9	4.7×10^4	1.2×10^{-7}

Notice that the time scale t is short enough so that rotation is probably not a dominant effect except at levels deeper than these. The values of T'/T show that the superadiabaticity is extremely

small. A time scale for horizontal mixing over a distance $L = 2 \times 10^8$ cm would be $t_L \sim L^2/K$. Evaluated at $p/p_0 = 1$, we find $t_L \sim 3.8 \times 10^7$ s ~ 1 year; notice that this is slightly shorter than the thermal time scale evaluated above.

4) In reality, latent heat effects would lead to a mean thermal structure somewhere between the moist and dry adiabats, if observations in the terrestrial atmosphere provide an accurate guide. The reason is that a moist adiabatic structure is actually stable because rising bubbles of moist material always entrain a certain amount of dry gas during their ascent through dry layers. For discussion, see e.g., Ooyama (1971). Unfortunately, our understanding of these processes is not complete enough to extend ideas to Jupiter and make predictions. Furthermore, molecular weight differences are much greater on Jupiter than on Earth, and are more important.

This completes our discussion of the hypothetical convective basic state. The important feature of the configuration is that it has adjusted itself to be only marginally unstable against perturbations on a dynamical (convective) time scale. We now proceed to argue that it would be unstable on a radiative time scale against certain large scale flows. We shall assume, although it is not crucial, that the basic state thermal structure is approximately given by the moist adiabat.

Consider the sequence of events:

- 1) A weak large scale flow develops, with downward motion at certain locations.

- 2) At these locations, dry gas now exists at the level where moist convection was previously occurring.
- 3) Convection ceases at these locations because the mean thermal structure is subadiabatic with respect to dry convection.
- 4) Radiative cooling continues at the tropopause level and therefore in the absence of convective heating from below, the locations with downwelling begin to cool, at all levels between the tropopause and the water cloud.
- 5) At locations with upwelling, the mean thermal structure remains unchanged. It is already close to the moist adiabat and cannot be heated further by convection.

On the average, then, there is a positive correlation between radiative heating rate and vertical displacement. Gierasch, Ingersoll, and Williams (1973) have shown that this can lead to instability. Gierasch (1973) shows that in equatorial regions, zonal symmetry is favored. For details, the reader is referred to these papers. We now list a few comments on the proposed instability.

- 1) The Gierasch, Ingersoll and Williams discussion assumed that vertical motion leads to increased infrared blanketing, and therefore radiative heating. An assumed static stability (subadiabatic structure) is necessary. The formulation is therefore self-consistent only if the circulation is seated at high levels in the atmosphere so that the motionless basic state is subadiabatic. Here we are proposing that the circulation extends down to the water cloud level, and we achieve a subadiabatic structure on the average because the moist adiabat is stable against dry convection.

2) The amplitude of the perturbation would be limited by the fact that $\Delta\theta$ could not exceed the difference between the moist and dry adiabats. For Jupiter, assuming a solar abundance of oxygen, this is $\Delta\theta \sim 1.7$ K (see Section IV, Table 2 for references and discussion). If we form a thermal wind equation by eliminating ϕ between (2) and (3), and then integrate from p_0 to p_1 , where p_1 is the observed cloud layer, we obtain

$$u(p_1) = - \frac{R}{f_0} \frac{\partial \bar{\theta}}{\partial y} \frac{1 - (p_1/p_0)^\kappa}{\kappa} \quad (32)$$

where we assumed $u(p_0) = 0$. Numerical values are presented in Section IV; for now we wish to point out how the scale of latitude variations might be determined. The radiative instability analyses showed that the smallest scales are favored. However, small scale belts and zones would be unstable on a short time scale to barotropic instability. The criterion is

$$\beta - \frac{\partial^2 u}{\partial y^2} \geq 0. \quad (33)$$

If we assume that $\Delta\theta$ does indeed always reach, but never exceed, the moist-dry adiabat difference, and if we assume that $u(p_1, y)$ is a smoothly varying function of y (as is suggested by the instability analyses in the linear regime), then we see that a scale is uniquely determined between (32) and (33). This result is consistent with Ingersoll and Cuzzi's (1969) discussion of Peek's (1958) data. The reasoning is obviously far from complete without detailed solutions, but nevertheless is suggestive.

3) The amplitude of the vertical motion field would be limited by the available heat flux. The heat flux is given by $F \sim \rho c_p w T'$, where w is the vertical velocity magnitude and T' is the temperature difference between rising and sinking gas. With

$$T' = \left(\frac{p}{p_0} \right)^{\kappa} \Delta\theta ,$$

and $\Delta\theta = 1.7$ K, we reach the numerical values listed in Table 2. We have used (29) and (30) to estimate diffusion coefficients and characteristic times for each level, although the interpretation is clearly different from the mixing length case, since a single large cell in the vertical is assumed. The important point is that motions are much slower in the present case, because a much larger temperature difference is introduced by the latent heat.

Table 2

Overturning rates for $\Delta\theta \sim 1.7$ K

The same parameter values are assumed as in Table 1.

p/p_0	$w(\text{cm s}^{-1})$	$K(\text{cm}^2 \text{s}^{-1})$	$t(\text{s})$	T'/T
0.1	0.33	6.6×10^5	6.1×10^6	3.2×10^{-3}
0.3	0.11	3.1×10^5	2.6×10^7	4.4×10^{-3}
1.0	0.033	1.3×10^5	1.2×10^8	6.2×10^{-3}

Notice that the time scale near the top is on the order of 60 days, whereas in the mixing length convection case it is about an hour. Using a length scale $L \sim 2 \times 10^8$ cm, we estimate a meridional velocity of about 30 cm s^{-1} , still smaller than the mixing length velocities even in spite of the large horizontal scale.

4) The overturning time and the growth rate for the belts and zones were estimated to be on the order of 10^8 s, while the horizontal diffusion time scale in deep layers was about half this. We therefore expect that the concentration of water vapor is influenced by the belt-zone circulation to appreciable degree at levels just below the cloud base, but very little at levels many scale heights below.

IV. Discussion

The general picture we have outlined is that Jupiter's belts and zones represent convection driven by the internal heat (and the fraction of the solar flux that penetrates to low levels). The phase change at the water cloud level provides a peculiar kind of interface across which rising currents undergo a temperature increment (relative to the dry adiabat). The thermal contrasts generated this way permit convection to carry the necessary heat flux with very slow motions compared to those mixing length theory would predict. The planetary vorticity gradient permits the shear associated with the axisymmetric belts and zones to be stable; this explains the symmetry and the length scale, as suggested by Ingersoll and Cuzzi (1969).

Concerning motions of short time scales we have suggested that inertial instabilities probably occur and maintain the Richardson number larger than unity. We have argued that barotropic shear instability occurs. Both these processes would lead to adjustments in the mean thermal field, and we showed that motions resulting from such adjustments would penetrate deep into the lower regions below the water cloud. It seems probable that when the sense of the vertical motion field is such as to draw moist gas upward, these sudden adjustments could lead to an eruption of spots along an entire belt or zone, and these events are indeed observed.

We wish now to ask what conditions are necessary for the existence of this kind of convection, and whether they are

met on the other outer planets also. We begin by evaluating several numerical parameters. Assume that the potential temperature gradient is given in the intermediate layer by

$$\frac{\partial \theta}{\partial y} = k \Delta \theta \sin ky, \quad (34)$$

where k is the latitudinal wavenumber. Then

$$\frac{\partial^2}{\partial y^2} u(p_1) = ak^3 u_0 \sin ky, \quad (35)$$

from (32) where

$$u_0 = \frac{R \Delta \theta}{f_0 a} \frac{1 - (p_1/p_0)^k}{k}, \quad (36)$$

is a thermal wind speed depending only on the planetary radius, a , and other physical parameters of the system. By substituting (35) into (33) we can solve for the critical wavenumber determined by the barotropic instability criterion, and then for the maximum wind speed U . We obtain

$$k^3 = \frac{\beta}{a u_0}, \quad U = a k u_0. \quad (37)$$

We tabulate (37) for Jupiter, Saturn, and Uranus in Table 3 below. The coriolis parameters f and β are evaluated at 30 degrees latitude. The tropopause and water cloud pressures p_1 and p_0 are based on the calculations presented by Weidenschilling and Lewis (1973). The value of $\Delta \theta$ is calculated from

$$\Delta \theta = \frac{x' L}{\mu c_p}, \quad (38)$$

where x' is the water vapor number fraction, L is the latent heat (4.7×10^{11} erg mole $^{-1}$), $\bar{\mu}$ is the mean molecular weight, and c_p is the heat capacity at constant pressure. For a solar mixture, $x' \approx 1.0 \times 10^{-3}$, $\bar{\mu} = 2.3$ gm mole $^{-1}$, $c_p = 1.3 \times 10^8$ erg K $^{-1}$ gm $^{-1}$, and we find $\Delta\theta \approx 1.7$ K.

We shall now calculate the ratio of vertical to horizontal potential temperature contrast, $\Delta\theta_v/\Delta\theta$, in the intermediate layer under the assumption that the Richardson number is unity, as suggested in Section II. The Richardson number is given by

$$Ri = \frac{\frac{g}{f} \left(\frac{\partial T}{\partial z} + \frac{g}{c_p} \right)}{\left(\frac{\partial u}{\partial z} \right)^2} = - \frac{f^2 \left(\frac{p_0}{p} \right)^\kappa p \frac{\partial \Theta}{\partial p}}{\left(\frac{\partial \Theta}{\partial y} \right)^2} \quad (39)$$

where z measures geometrical height and the hydrostatic relation has been used to transform to the right hand expression. Assuming that $\partial \Theta / \partial y$ is independent of height (which is consistent only if $\Delta\theta_v \ll \Delta\theta$), and assuming that the maximum value of $\partial \Theta / \partial y$ is $k\Delta\theta$, we can solve (39) for $\partial \Theta / \partial p$ and integrate to obtain the maximum vertical potential temperature contrast. We obtain

$$\frac{\Delta\theta_v}{\Delta\theta} = \frac{k^2 R \Delta\theta}{f_0^2} \frac{1 - (p_1/p_0)^\kappa}{\kappa} = \epsilon, \quad (40)$$

where $\epsilon = kU/f$. This verifies the estimate made in Section II, at least for one particular structure assumption.

We see that as we move from Jupiter to Saturn to Uranus, assuming solar composition, both the wavelength-radius ratio and the Rossby number become larger. If these numbers approach

Table 3

Dynamical parameters and cloud levels

The first three rows present data, based on Weidenschilling and Lewis (1973). H is the scale height at the water cloud temperature Θ . The next three rows present derived quantities as discussed in the text. The wavelength $\lambda = 2\pi/k$. Quantities in parenthesis for Saturn and Uranus are based on water abundances 2 and 5 times the solar composition value respectively. In all cases, $f_0 = 1.7 \times 10^{-4} \text{ s}^{-1}$ and $c_p = 1.3 \times 10^8 \text{ erg K}^{-1} \text{ gm}^{-1}$.

	$a(10^8 \text{ cm})$	$g(\text{cm s}^{-2})$	Θ	$H(\text{km})$	$p_0(\text{atm})$	p_1/p_0	$\beta(\text{cm}^{-1} \text{ s}^{-1})$
Jupiter	70	2400	275	43	7	14	4.2×10^{-14}
Saturn	60	1000	290	107	20	40	4.9×10^{-14}
Uranus	22	900	360	143	150	500	1.3×10^{-13}

	$u_0(\text{ms}^{-1})$	$U(\text{ms}^{-1})$	$\lambda(10^8 \text{ cm})$	λ/a	ϵ
Jupiter	1.0	28	16	.23	.06
Saturn	1.4 (2.8)	33 (52)	16 (20)	.27 (.33)	.09 (.10)
Uranus	4.5 (22)	50 (150)	12 (21)	.56 (.94)	.15 (.26)

unity we expect qualitatively different behavior for either geometrical or dynamical reasons. The principal parameter causing the increase is the decreasing planetary radius. In particular, λ/a exceeds one-half for Uranus. (We have assumed, of course, that there are internal heat sources or sufficiently deep penetration of sunlight to drive motions.)

Motions predicted on Saturn are only slightly stronger than on Jupiter, for solar composition. Observations suggest, however, that motions may be several times stronger (Moore, 1939). The only explanation consistent with the ideas proposed here is that the O:H ratio is higher on Saturn. We have shown approximate values of derived parameters for Saturn and Uranus atmospheres enriched 2 and 5 times, respectively, relative to solar composition.

Notice that because the latitudinal scale is determined by the barotropic instability criterion, the last two columns in Table 3 are related. In fact, since $\beta \sim \Omega/a$, we have $\epsilon \sim (ka)^{-1}$.

Two comments can be made regarding the great red spot and the equatorial jet. Our ideas here are consistent with Ingersoll's (1973) suggestion that the red spot is a free atmospheric vortex. As he points out, once it is known that the barotropic vorticity equation governs the flow, the question becomes one of initial conditions. We add one more question here: Can a vertical circulation pattern exist inside the spot to maintain the horizontal $\Delta\theta$ necessary to provide the anti-cyclonic motion?

The equatorial jet could be maintained by equatorward momentum transport in two-dimensional eddies governed by the same equation. Gierasch (1975) has made a similar suggestion regarding momentum transports in the Venus atmosphere. This question should be susceptible to numerical study.

A number of other theoretical questions are raised by the conjectures we have made in this paper. One hesitates to

make a long list when the observational basis is so meager. Two, however, are worth mentioning. We have assumed here that deep layers are horizontally uniform in composition and temperature. What really is the nature of the coupling between the deep and intermediate layers? How do moisture and molecular weight affect small scale convection near the interface? Does a large scale circulation indeed suppress moist convection? The second question is an easier one: Can the horizontal temperature gradients we postulate in the intermediate layer be stable? Does the presence of the deep layer suppress baroclinic instabilities?

Observational questions related to these ideas are obvious and we shall mention only a few. More details of the motion field at cloud level would be extremely useful, to determine whether small scales of motion (possibly related to inertial instabilities) exist, and to what accuracy the flow really is governed by vorticity conservation. The thermal structure near the cloud tops is important. Composition variations (both water and other condensing constituents) may be extreme between zones and belts. Is the concentration greatest in zones? How deep do variations extend? Thermal contrasts in intermediate and deep layers are highly desirable but probably hopeless to obtain, since variations from adiabatic (both horizontally and vertically) are on the order of 1K.

Acknowledgments

This work has been supported in part by NASA Grant NGL-33-010-186, and by an Alfred P. Sloan Foundation research fellowship. The author is grateful to both agencies.

References

- Barcilon, A., and P. J. Gierasch, 1970: A moist Hadley cell model for Jupiter's cloud bands. J. Atmos. Sci., 27, 550-560.
- Bogart, R. S., and P. J. Gierasch, 1976: Mixing length theory and lateral heat transport. In preparation.
- Gierasch, P. J., 1973: Jupiter's cloud bands. Icarus, 19, 482-494.
- Gierasch, P. J., 1975: Meridional circulation and the maintenance of the Venus atmospheric rotation. J. Atmos. Sci., 32, 1038-1044.
- Gierasch, P. J., A. P. Ingersoll, and R. T. Williams, 1973: Radiative instability of a cloudy planetary atmosphere. Icarus, 19, 473-481.
- Ingersoll, A. P., 1973: Jupiter's great red spot: a free atmospheric vortex? Science, 182, 1346-1348.
- Ingersoll, A. P., and J. N. Cuzzi, 1969: Dynamics of Jupiter's cloud bands. J. Atmos. Sci., 26, 981-985.
- Ingersoll, A. P., G. Munch, G. Neugebauer, and G. S. Orton, 1975b: Results of the infrared radiometer experiment on Pioneers 10 and 11. Paper presented at the Jupiter conference in Tucson on May 20, 1975.
- Ingersoll, A. P., G. Munch, G. Neugebauer, D. J. Diner, G. S. Orton, B. Schupter, M. Schroeder, S. C. Chase, R. D. Ruiz and L. M. Trafton, 1975a: Pioneer II infrared radiometer experiment: The global heat balance of Jupiter. Science, 188, 472-473.

- Maxworthy, T., and L. G. Redekopp, 1975: A solitary wave theory of the great red spot and other features in the Jovian atmosphere. Paper presented at the Jupiter conference in Tucson on May 20, 1975.
- McIntyre, M. F., 1970: Diffusive destabilization of the baroclinic circular vortex. Geophys. Fluid Dyn., 1, 19-57.
- Ooyama, K., 1971: V. Convection and convective adjustment: A theory on parameterization of cumulus convection. J. Met. Soc. Japan, 49, 744-756.
- Peek, B. M., 1958: The Planet Jupiter. Faber and Faber, London.
- Rossow, W. B., and P. J. Gierasch, 1976: Cloud properties on the planets. In preparation.
- Stone, P. H., 1966: On non-geostrophic baroclinic instability. J. Atmos. Sci., 23, 390-400.
- Stone, P. H., 1967: An application of baroclinic stability theory to the dynamics of the Jovian atmosphere. J. Atmos. Sci., 24, 642-652.
- Stone, P. H., 1971: The symmetric baroclinic instability of an equatorial current. Geophys. Fluid Dyn., 2, 147-164.
- Stone, P. H., 1975: The meteorology of the Jovian atmosphere. Paper presented at the Colloquium on Jupiter, Tucson, Arizona, May 18-23, 1975. To appear in Jupiter, The Giant Planet, T. Gehrels, Ed., U. Arizona Press.
- Weidenschilling, S. J., and J. S. Lewis, 1973: Atmospheric and cloud structures of the Jovian planets. Icarus, 20, 465-476.
- Williams, G. P., 1975: To appear in Nature.

Figure Captions

Figure 1. The three layers. An approximate temperature profile is indicated, with the moist adiabat sketched in as a dashed line.

Figure 2. Development of belts and zones. In the initial configuration convection occurs at all levels as indicated by the stippling. During growth, convection ceases near the water cloud level at locations of large scale downwelling. The final configuration has no small scale convection above the water cloud because the intermediate layer is stabilized as discussed in Section II.

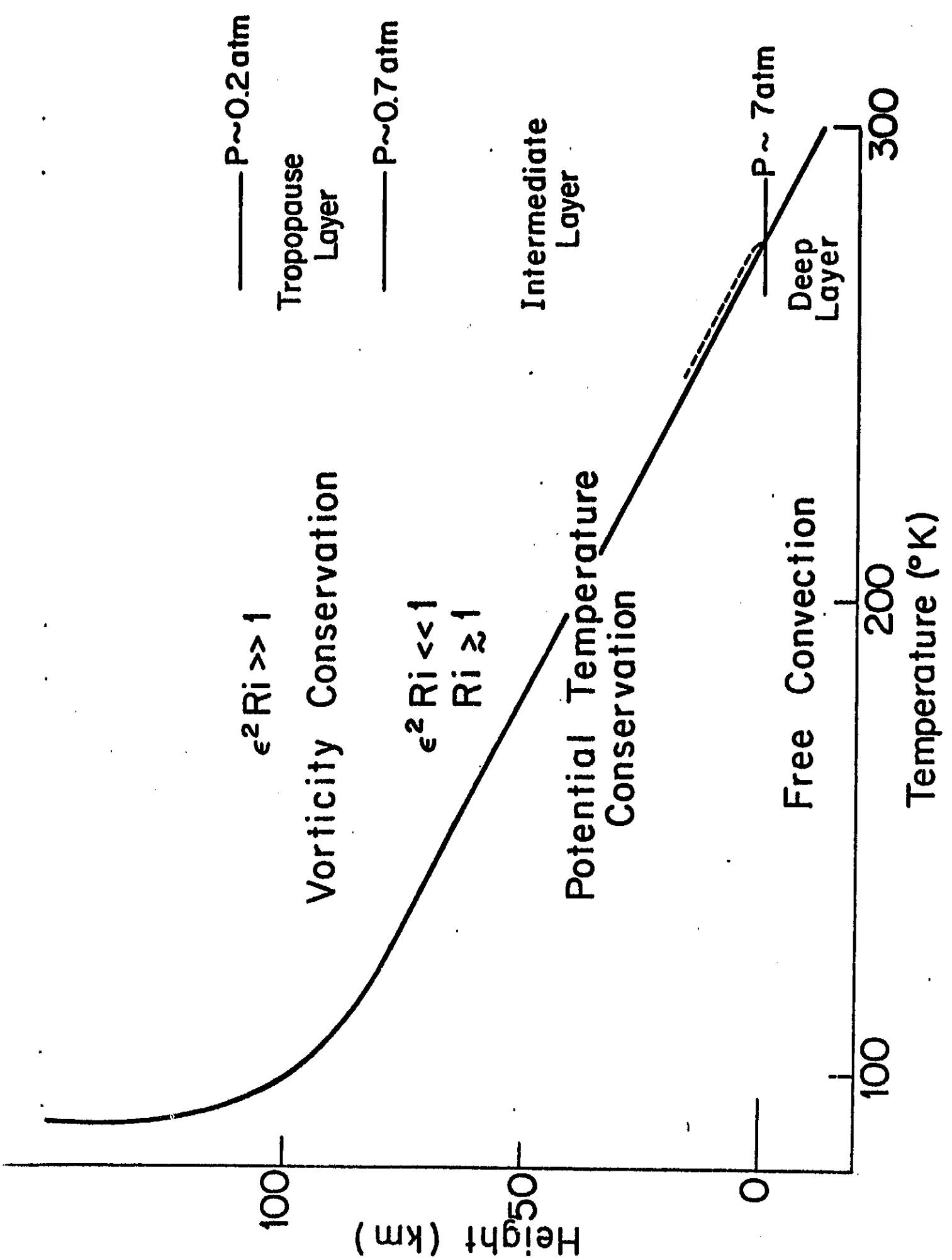
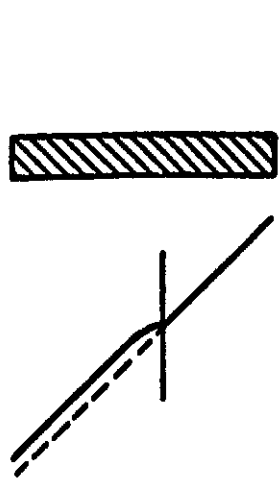
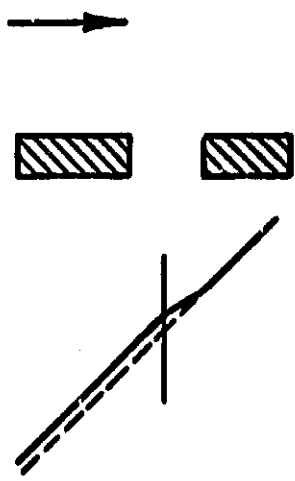


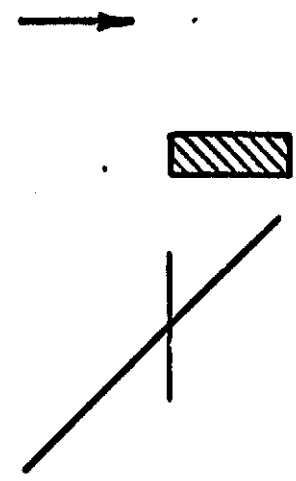
Figure 1



Initial

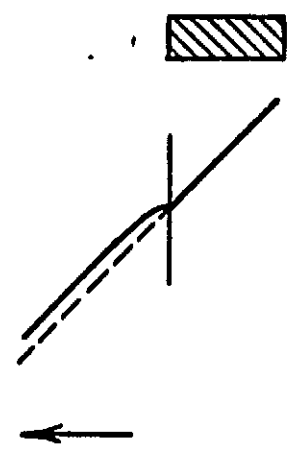
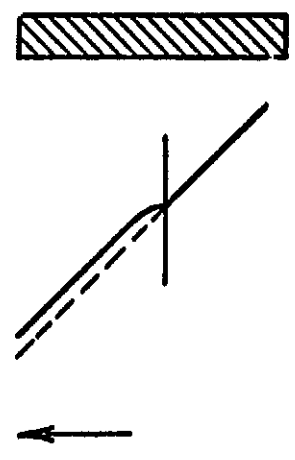
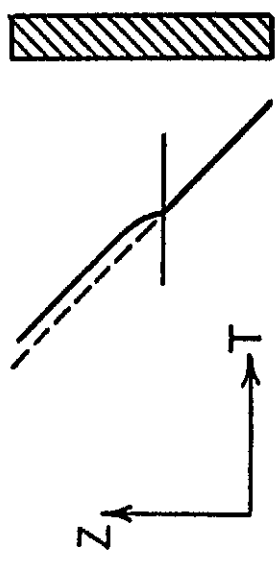


Growth



Final

Belt



Zone

Figure 2